Surfactant effect on the ultrafiltration of oil-in-water emulsions using ceramic membranes

María Matos, Gemma Gutiérrez, Alberto Lobo, José Coca, Carmen Pazos, José M. Benito

www.elsevier.com/locate/memsci

PII: S0376-7388(16)31386-2
DOI: http://dx.doi.org/10.1016/j.memsci.2016.08.037
Reference: MEMSCI14687

To appear in: *Journal of Membrane Science*

Received date: 29 April 2016
Revised date: 18 August 2016
Accepted date: 21 August 2016

Cite this article as: María Matos, Gemma Gutiérrez, Alberto Lobo, José Coca Carmen Pazos and José M. Benito, Surfactant effect on the ultrafiltration of oil in-water emulsions using ceramic membranes, *Journal of Membrane Science* http://dx.doi.org/10.1016/j.memsci.2016.08.037

Surfactant effect on the ultrafiltration of oil-in-water emulsions using ceramic membranes

María Matos[a], Gemma Gutiérrez[a], Alberto Lobo[a], José Coca[a], Carmen Pazos[a], José M. Benito[b*]

[a]Department of Chemical and Environmental Engineering, University of Oviedo, C/ Julián Clavería 8, 33006 Oviedo, Spain

[b]Department of Biotechnology and Food Science. University of Burgos. Plaza Misael Bañuelos s/n, 09001 Burgos, Spain

[*]Corresponding author. Tel.: +34-947258810; fax: +34-947258831. E-mail address: jmbmoreno@ubu.es (José M. Benito)

Abstract

Ultrafiltration (UF) of oil-in-water (O/W) emulsions formulated with 1 wt. % base oil (an 85/15% (w/w) mixture of a synthetic poly-α-olefin and trimethylol propane trioleate ester, respectively), and a surfactant (anionic, Oleth-10, nonionic, Brij 76, or cationic, CTAB) at several concentrations referred to its critical micelle concentration (CMC) was studied using two different cut-off (50 and 300 kDa) tubular ceramic membranes.

Effect of O/W emulsion (surfactant type and its concentration, zeta potential, oil droplet size, pH) and membrane (pore size, surface charge) characteristics on UF process were also investigated. Permeate flux and chemical oxygen demand (COD) in permeate were determined for each emulsion. COD rejections higher than 95% were achieved for both membranes.

An UF model of nonionic surfactant-stabilized O/W emulsion was developed based on an osmotic pressure model and a mass transfer model (film theory) by defining two types of rejection for free monomers and micelles of surfactant (Model A). Permeate fluxes were adequately predicted for both membranes, while solute concentration in permeate showed large discrepancies, especially for 50 kDa membrane. Prediction was improved for both membranes when three new parameters were used in a second model (Model B), taking into account diffusion and convection inside membrane pores.

Keywords: Oil-in-water emulsion; Ultrafiltration; Ceramic membrane; Surfactant; Modeling

Nomenclature

List of symbols

C_b	surfactant concentration in bulk solution (mol L^{-1})
C_m	surfactant concentration at membrane surface (mol L^{-1})
C_{mic}	concentration of micelles (mol L^{-1})
$C_{mic,m}$	micelles concentration on membrane surface (mol L^{-1})
C_{mon}	concentration of surfactant monomers (mol L^{-1})
C_p	surfactant (solute) concentration in permeate (mol L^{-1})
C_s	total surfactant concentration (mol L^{-1})
CMC	critical micelle concentration (mol L^{-1})
D	solute diffusion coefficient (m^2 s^{-1})
$D_{[4,3]}$	volume mean diameter of oil droplets (μm)
J	permeate flux (m s^{-1})
J_{crit}	critical flux (m s^{-1})
J_s	solute flux (m s^{-1})
J_x	permeate flux as a function of membrane length (m s^{-1})
k	mass transfer coefficient (m s^{-1})
K_c	hindrance factor for convective flux
K_d	hindrance factor for diffusive flux
L	membrane channel length (m)
L_p	pore length (m)
n_{aggr}	aggregation number of surfactant
Pe_m	membrane Peclet number, defined by Eq. (13)
R	ideal gas constant (8.314 J mol^{-1} K^{-1})
R_c	cake layer resistance (m^{-1})
R_{int}	intrinsic rejection
R_m	intrinsic membrane resistance (m^{-1})
R_{mic}	micelle rejection
R_{mon}	monomer rejection
S_a	actual sieving coefficient, defined by Eq. (12)
S_∞	high flux asymptotic sieving coefficient, defined by Eq. (14)
T	absolute temperature (K)
x/L	dimensionless membrane channel length

Greek letters

ΔP	transmembrane pressure, TMP (MPa)

ϕ equilibrium partition coefficient

ϕ_{mic} equilibrium partition coefficient for the micelles

Φ_{mic} micelle volumetric fraction

λ ratio between solute radius and membrane pore radius

λ_{mon} ratio between surfactant monomer radius and membrane pore radius

μ viscosity (MPa s)

Π osmotic pressure (MPa)

1. Introduction

Metalworking fluids (MWFs) are oil-in-water (O/W) emulsions commonly used as lubricants and coolants in metal-finishing industries. These emulsions are a complex mixture of water, oil and additives, such as surfactants, corrosion inhibitors, and antifoaming agents. MWFs lose their functional properties with use, resulting in large volumes of oily wastewater that need to be treated before disposal [1–3].

Each effluent may require a specific oil/water separation process, depending on physical nature of the oil, oil content, and chemical nature of other components. The most common treatment methods are chemical destabilization (coagulation/flocculation), electrocoagulation [4], centrifugation [5,6], membrane filtration [2,7–12], and vacuum evaporation [2,13–15]. Membrane filtration is a suitable technique for treating oily wastewaters because of the high quality of the permeate (i.e. low chemical oxygen demand, COD).

However, membranes suffer a permeate flux decline over time due to concentration polarization and fouling as a result of adsorption and accumulation of rejected oil and other components on the membrane surface [12,16]. This leads to high energy consumption and frequent membrane cleaning requirements that shortens membrane lifetime. To reduce fouling and reach better process efficiency, several techniques have been coupled with membrane processes for the treatment of oily wastewater [17–25]. The higher quality of these final effluents (permeates) could make them suitable for recirculation as process water or for MWF reformulation depending on their surfactant content [26,27].

Ceramic ultrafiltration (UF) membranes are increasingly used in the treatment of oily water streams because of their higher mechanical, chemical and thermal stability. Their active layer is usually formed by metallic oxides that can exist in different ionization states or zeta potential values depending on pH and ionic strength of the feed.

Several mathematical models have been used to explain the permeate flux decline due to concentration polarization and particle (oil droplets in this case) deposition on the membrane surface. Most of them are based on the balance of forces acting on particles and they define a critical flux depending on ionic strength, zeta potential, and particle size [28,29]. However, the membrane operation becomes more complicated when surfactants are present. At a certain concentration known as critical micelle concentration (CMC), the surfactant associates into micelles: hydrophilic groups are oriented towards the bulk aqueous phase whilst hydrophobic groups remain inside the micelles. These micelles can entrap oil droplets to form an O/W emulsion. At concentrations higher than CMC, monomers and micelles coexist in equilibrium. It has been reported that surfactant monomers either decrease or enhance permeate flux because they tend to adsorb onto the membrane surface due to electrostatic forces or hydrophobic effects [8,20]. The extent of this adsorption depends on surfactant type (anionic, nonionic or cationic) and membrane surface properties. Adsorption of surfactants onto membrane surface leads to two different effects: decline of permeate flux as a result of effective membrane pore radius reduction, and changes in the membrane surface (basically by electrostatic and hydrophobic/hydrophilic interactions). A modification of membrane characteristics affects concentration polarization, membrane fouling, and solute retention leading to changes in flux and COD of the permeate [8,20].

Several authors have reported flux reduction with concentration polarization and osmotic pressure enhancement due to accumulation of charged colloids near the membrane. Osmotic pressure is affected by parameters such as zeta potential, ionic strength, pH, and particle radius. Furthermore, other authors suggest that at a certain concentration a cake layer is formed on the membrane surface, causing a resistance to the flux that is proportional to its specific resistance and thickness. The specific resistance and thickness of the cake layer depends on particle-particle and particle-membrane interactions, which are influenced by the same parameters as osmotic pressure [28–31]. This model likely applies to emulsion ultrafiltration since oil droplets can coalesce near the membrane.

The aim of this work was to study the UF of O/W emulsions made up of base oil and a surfactant (anionic, nonionic, or cationic) at various concentrations, referred to its CMC. Zeta potential and droplet size of the formulated emulsions were measured. Two UF tubular ceramic membranes were used in this work. Permeate fluxes and COD values were also determined. UF modeling of O/W emulsions stabilized with the nonionic surfactant (to avoid the influence of electrostatic interactions) was performed using an osmotic pressure model and a mass transfer model (film theory). Two types of rejection were assumed, on the basis that surfactants are present both as free monomers and micelles, whereas in an extension of the model, three new adjustment parameters were used to account for diffusion and convection phenomena inside the membrane pores.

2. Materials and methods

2.1. Emulsion formulation

O/W emulsions were formulated using an 85/15% (w/w) mixture of a synthetic poly-α-olefin (PAO-6, Repsol, Spain) and trimethylol propane trioleate ester (Fuchs Lubricantes, Spain), respectively, as base oil, with a density of 0.897 g/L. Three surfactants, supplied by Sigma–Aldrich Co. (Germany) with purities higher than 99%, were added to stabilize the emulsion: Oleth-10 (glycolic acid ethoxylate oleyl ether, anionic, CMC = 20 mg/L), Brij 76 (polyethylene glycol octadecyl ether, nonionic, CMC = 200 mg/L), and CTAB (hexadecyltrimethyl ammonium bromide, cationic, CMC = 350 mg/L). Their CMC were determined at 20 ºC by surface tension measurements using a Krüss K-8 tensiometer (Germany), with the Du Noüy platinum ring method [32].

All the emulsions were prepared with 1% (w/w) base oil in deionized water (Millipore Elix 5 deionizer, USA) and varying surfactant concentrations: 0.25, 0.5, 1, 2, and 10 times the CMC. First, the base oil was blended with the surfactant by stirring on a hot plate at the desired concentrations. This concentrate was then dispersed in deionized water using a homogenizer Heidolph DIAX 900 (Germany), at 15,000 rpm for 10 min.

2.2. Emulsion characterization

Droplet size distributions (DSD) of the O/W emulsions were measured by laser diffraction using a Malvern Mastersizer S long bench equipment (Malvern Instruments Ltd., UK). The emulsions were previously diluted with deionized water (1:10 dilution ratio) to prevent multiple scattering effects.

A Malvern Zetasizer Nano ZS (Malvern Instruments Ltd., UK) was used to measure the electrophoretic mobility of O/W emulsions by laser Doppler microelectrophoresis, and then to determine their zeta potential by application of the Henry equation and Smoluchowski approximation. No dilution of O/W emulsions was required.

Emulsions pH was determined at room temperature using a Crison Basic 20 pH-meter (Crison, Spain).

Zeta potential and average oil droplet size (volume mean diameter, $D_{[4,3]}$) of fresh O/W emulsions as a function of surfactant concentration are shown in Fig. 1.

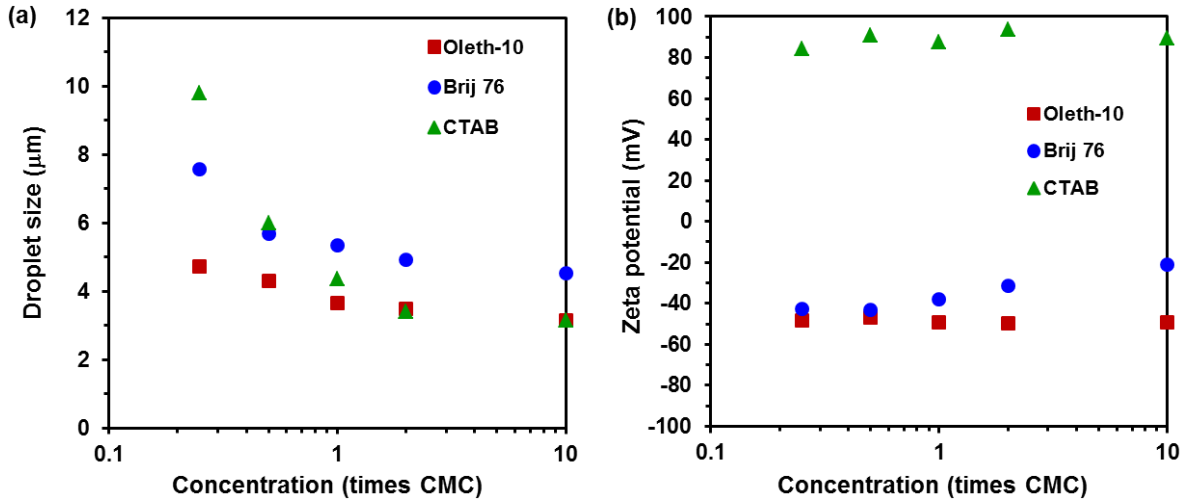

Figure 1. O/W emulsion characteristics at different surfactant concentrations: (a) average oil droplet size (volume mean diameter, $D_{[4,3]}$), and (b) zeta potential.

2.3. Ultrafiltration experiments

Two Carbosep® trilobe tubular ceramic membranes (Rhodia Orelis, Miribel, France) were used in this study (Carbosep M308 and Carbosep M309). They have an active layer of ZrO_2/TiO_2 supported on carbon, with molecular weight cut-off (MWCO) of 50 and 300 kDa, respectively. The tubular membranes are of 1200 mm length and 10 mm outer diameter, with three 3.6 mm internal diameter channels and a total filtration area of 0.05 m^2.

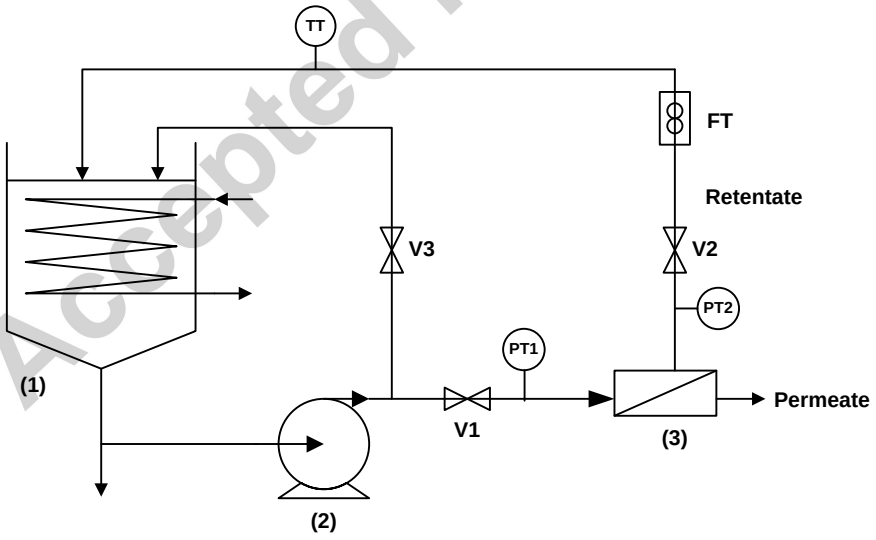

Figure 2. Schematic diagram of the UF equipment.

The UF experimental device is shown in Fig. 2. The feed solution was circulated by a Grundfos CHI4 (Spain) centrifugal pump (2) from a 15 L internally-cooled feed tank (1) to the

membrane module (3). The circulation flow rate was measured using a Comaquinsa R-005 Inox (Spain) flowmeter (FT), and the permeate flux was measured volumetrically. Crossflow velocities and transmembrane pressures (TMP) were monitored by flow control valves (V1, V2, and V3). The operating variables were kept constant during the experiment, and measured by pressure (PT1, PT2) and temperature (TT) transducers.

Experiments were conducted in total recycle mode (i.e. both retentate and permeate were returned to the feed tank) at 25.0±0.5 ºC and in a TMP range of 0.05–0.4 MPa. The steady state operation was quickly reached. Each experimental run took no more than 20 min to completion, except for CTAB surfactant experiments, where more time was needed to reach steady state. Experiments were performed at 3.4 m s^{-1} of crossflow velocity and at the aforementioned surfactant concentrations. Permeate samples were withdrawn for each TMP after 20 min of operation and COD values of permeate and retentate were measured.

2.4. Membrane cleaning procedure

The membrane was cleaned after each experiment following a two-stage procedure: first, it was cleaned with 1 vol. % Derquim+ (commercial detergent supplied by Panreac, Spain) in deionized water during 45 min at 40 ºC, 0.1 MPa, and a crossflow velocity of 5 m/s. Then, it was rinsed with deionized water and cleaned again using a 0.3 vol. % HNO_3 aqueous solution at 40 ºC, 0.1 MPa, and 5 m s^{-1} during 45 min. After this second stage, the membrane was rinsed again with freshly deionized water and the permeate flux was measured at 20 ºC and different TMPs and compared to the initial water flux of the new membrane.

2.5. Permeate characterization

Solute retention in the UF process was determined by COD analysis of both permeate and retentate by the reactor digestion method [33] using a HACH DR2010 UV spectrophotometer (USA).

2.6. UF modeling of O/W emulsions stabilized with a nonionic surfactant (Brij 76)

Micelles are surfactant aggregates, usually of spherical shape, formed above the CMC. The radii of spherical micelles usually are in the range of 1–10 nm and can be considered macromolecular solutions. Several models have been proposed to predict the UF of macromolecular solutions, such as gel-polarization, osmotic pressure, and resistances-in-series. Some authors have neglected the role of osmotic pressure on the UF of

macromolecules, but at high concentrations the osmotic pressure increases exponentially and may become as high as 250 kPa for surfactant solutions [34]. When surfactant micelles are rejected by the membrane, a concentration gradient develops in the boundary layer and local concentration at membrane surface may be 300 times higher than in bulk solution, depending on polarization layer thickness. Hence, osmotic pressure increases leading to a reduction in the effective TMP. A combination of van't Hoff and Carnahan-Starling equations may be used to estimate the osmotic pressure of surfactants for weak electrostatic interactions between micelles [31]:

$$\Pi = RT\left(C_{\text{mon}} + C_{\text{mic}}\left(\frac{1+\Phi_{\text{mic}}+\Phi_{\text{mic}}^2-\Phi_{\text{mic}}^3}{(1-\Phi_{\text{mic}})^3}\right)\right) \quad (1)$$

where R is the ideal gas constant (8.314 J mol^{-1} K^{-1}), T is the absolute temperature (K), C_{mon} (mol L^{-1}) is the concentration of surfactant monomers, C_{mic} (mol L^{-1}) is the concentration of micelles, and Φ_{mic} is the micelle volumetric fraction. The total surfactant concentration, C_s (mol L^{-1}), can be calculated as:

$$C_s = C_{\text{mon}} + n_{\text{aggr}} C_{\text{mic}} \quad (2)$$

where n_{aggr} is the aggregation number of surfactant, i.e., number of surfactant monomers per micelle. In this work, n_{aggr} = 90 was assumed, since it is a typical value for nonionic surfactants. CMC was experimentally determined (2.8×10^{-4} mol L^{-1}) as explained in Section 2.1. A micelle radius of 4.6 nm, obtained from Dynamic Light Scattering (DLS) measurements using the Malvern Nano ZS apparatus, was required to calculate the volume occupied by a micelle and therefore Φ_{mic}.

In the film theory, the convective transport of solute to the boundary layer is equal to permeate flux and diffusive back transport of solute into the bulk solution. Assuming that the diffusion coefficient is independent of concentration, permeate flux is given as a function of mass transfer coefficient, k [30,31,34]:

$$J = k \ln\left(\frac{C_m - C_p}{C_b - C_p}\right) \quad (3)$$

where C_m (mol L^{-1}) is the surfactant concentration at membrane surface, C_b (mol L^{-1}) is the surfactant concentration in the bulk solution, and C_p (mol L^{-1}) is the surfactant (solute)

concentration in the permeate. The mass transfer coefficient, k (m s^{-1}), can be estimated by the Sherwood correlation for tubular geometries and can be expressed as a function of the dimensionless membrane channel length, x/L [35]:

$$k = k_0 \left(\frac{x}{L} \right)^{1/3} \quad (4)$$

where k_0 is a constant that depends on the kind of flow (laminar or turbulent) inside membrane channel [25,35].

In the osmotic pressure model, permeate flux (J) is given by the following equation:

$$J = \frac{\Delta P - \Delta \Pi}{\mu R_m} \quad (5)$$

where ΔP (MPa) is the TMP, $\Delta\Pi$ (MPa) is the osmotic pressure difference between membrane surface and permeate, μ is the viscosity (MPa s), and R_m (m^{-1}) is the intrinsic membrane resistance that can be determined from pure water fluxes at different TMPs.

Eqs. (1-5) can be solved simultaneously to obtain C_m and J. However, the surfactant membrane rejection is needed to determine C_p. At this point, two different types of rejection must be defined taking into account that surfactants are present both as free monomers and micelles. These are R_{mon} and R_{mic}, which correspond to monomer rejection and micelle rejection, respectively. The following equation is then applied to obtain the actual or so-called intrinsic rejection, R_{int} [31]:

$$R_{int} = 1 - \frac{C_p}{C_m} = 1 - \frac{n_{aggr} C_{mic} (1 - R_{mic}) + CMC (1 - R_{mon})}{C_m} \quad (6)$$

If the concentration on the membrane surface is smaller than CMC, R_{int} would be equal to R_{mon} since micelles are not formed.

For a tubular membrane, permeate flux varies with membrane length and therefore TMP and mass transfer coefficient also change. Crossflow velocity was kept constant at 3.4 m s^{-1} for all UF experiments in this study. The corresponding TMP drops with membrane length were 0.1 MPa m^{-1} for the 300 kDa membrane and 0.06 MPa m^{-1} for the 50 kDa one. Permeate flux is then given by the following equation:

$$J = \frac{1}{L}\int_0^L J_x \mathrm{d}x \qquad (7)$$

where J (m s^{-1}) is the steady-state permeate flux and J_x (m s^{-1}) is the permeate flux as a function of membrane length.

Surfactant (solute) concentrations in permeate were obtained by dividing solute flux (J_s) by permeate flux (J). J_s was also calculated by integrating flux across membrane length, and surfactant concentration in permeate, C_p, is given by:

$$C_p = \frac{J_s}{J} = \frac{\frac{1}{L}\int_0^L J_x C_p \, \mathrm{d}x}{J} \qquad (8)$$

Emulsions also have oil droplets that can be located at membrane surface when the flux obtained (J) is higher than critical flux (J_{crit}). In that case, an additional resistance (R_c) should be taken into account due to the cake layer formed and Eq. (5) is given as:

$$J = \frac{\Delta P - \Delta \Pi}{\mu(R_m + R_c)} \qquad (9)$$

The critical flux is defined as the permeate flux above which fouling appears. It is possible that in certain membrane regions J_{crit} can be reached because of fouling, while in other parts of the membrane permeate flux just decreases by concentration polarization or even by the increase in osmotic pressure caused by surfactant accumulation.

3. Results and discussion

3.1. UF of O/W emulsions stabilized by surfactants

Figs. 3 and 4 show the effect of TMP on the steady-state permeate flux (J) for the UF of the O/W emulsion stabilized with varying concentrations of the anionic (Oleth-10), nonionic (Brij 76) and cationic (CTAB) surfactants, using 50 kDa and 300 kDa ceramic membranes, respectively.

For the anionic surfactant-stabilized O/W emulsions, permeate flux increased steadily with TMP for the 50 kDa membrane (Fig. 3a): a flux decline was observed as the anionic surfactant concentration increased close to its CMC and then it remained constant. This flux

reduction was even more noticeable for the 300 kDa membrane (Fig. 4a). Permeate fluxes for both membranes were very similar at high anionic surfactant concentrations. Nevertheless, for the 300 kDa membrane, permeate flux did not increase linearly with TMP at high anionic surfactant concentrations because of concentration polarization. This behavior is more noticeable in membranes with large pore size. Initial water flux is higher and solutes (in this case micelles and oil droplets) accumulate near the membrane surface by convective flux, causing an additional resistance [30,31] and a cake layer build-up when permeate flux is higher than the critical flux. It should be pointed out that fluxes did not vary linearly with TMP for UF of the emulsion without surfactant, being especially noticeable for the 300 kDa membrane: oil droplets were not stabilized by the surfactant and consequently they tend to deposit, and even to coalesce at the highest TMP tested, on the membrane surface [36].

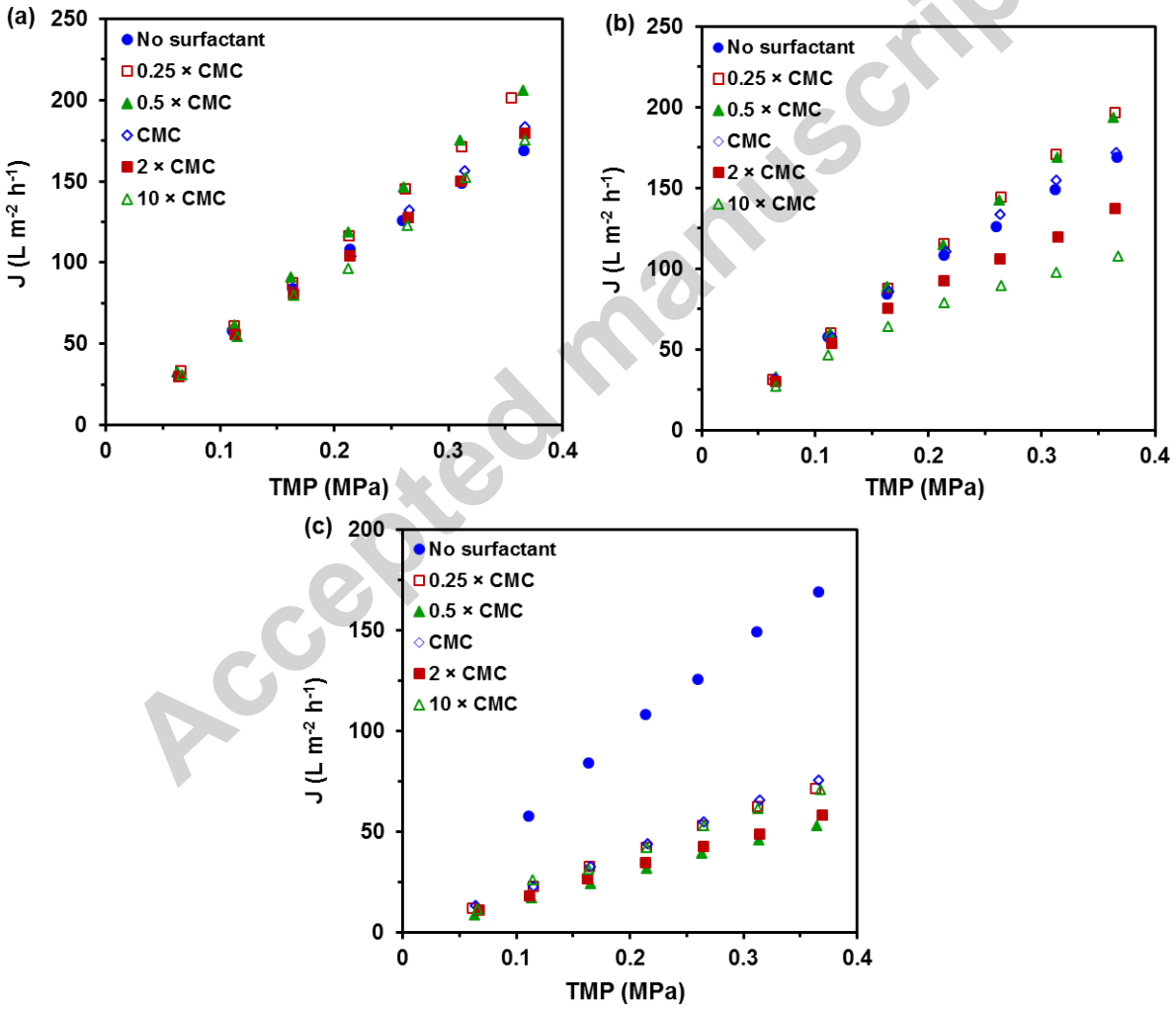

Figure 3. Permeate flux at different TMP and surfactant concentration using a 50 kDa ceramic membrane for UF of a model O/W emulsion formulated with: (a) Oleth-10, (b) Brij 76, and (c) CTAB surfactant.

When anionic surfactant concentration is lower than CMC, surfactant monomers are adsorbed at oil/water interface or on membrane surface. The ZrO_2/TiO_2 active layer of the membranes exhibits different ionization states or zeta potential values depending on pH [37]. Isoelectric point for this kind of membranes can be estimated by streaming potential measurements with a value close to 4 [38]. The pH of the anionic surfactant-stabilized emulsions used in this work was about 6.5, which means that the membrane is negatively charged (ZrO^-/TiO^-). This fact, along with the high negative value of zeta potential shown in Fig. 1, indicates that electrostatic repulsion between oil droplets and membrane surface did not further lower the flux because of anionic surfactant adsorption on the membrane.

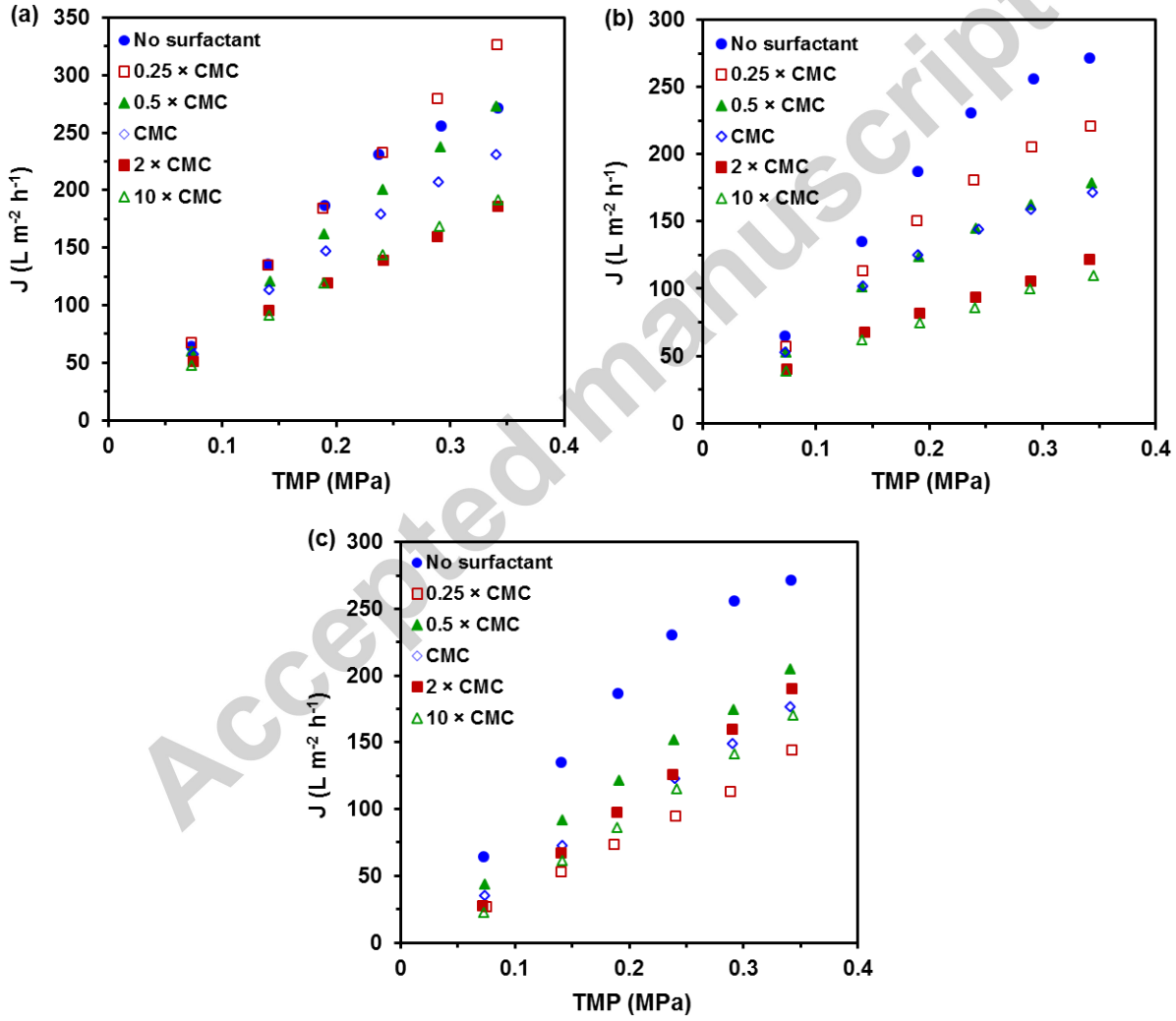

Figure 4. Permeate flux at different TMP and surfactant concentration using a 300 kDa ceramic membrane for UF of a model O/W emulsion formulated with: (a) Oleth-10, (b) Brij 76, and (c) CTAB surfactant.

Permeate fluxes as a function of TMP for the UF of O/W emulsion stabilized with varying concentrations of the nonionic surfactant (Brij 76) are shown in Figs. 3b and 4b. Fluxes did not increase steadily with TMP due to the large effect of concentration polarization. Again, concentration polarization had a stronger influence on the 300 kDa than on the 50 kDa membrane. As shown in Fig. 1, zeta potential absolute values of nonionic surfactant-stabilized emulsions are lower and droplet size is higher than those obtained for the ionic surfactant-stabilized ones. Hence, repulsion between oil droplets is lower and they tend to accumulate near the membrane surface, especially at high fluxes [8,23,24]. Above a certain concentration, a cake layer is formed on the membrane, which results in an additional resistance to permeation. Since a raise in TMP increases the concentration at the membrane surface because of the enhanced mass transport to the membrane, the resistance to permeation also increases with pressure. Furthermore, the specific resistance of the cake layer increases when particle size decreases, which explains the concentration polarization effect observed, especially at high nonionic surfactant concentrations.

It is observed in Fig. 4b that fluxes for the 300 kDa membrane, at high TMP and surfactant concentration, are slightly lower than for the 50 kDa membrane (Fig. 3b). Lower fluxes for higher pore size membranes have been observed by other authors [39]. It may be attributed to constriction of pores (or internal fouling) in higher pore size membrane, in addition to the external fouling that occurs in both membranes. For the 50 kDa membrane, permeate fluxes increased with respect to the base oil with the addition of Brij 76, but as nonionic surfactant concentration increased fluxes decreased until a concentration of 2 $\times$ CMC was reached, at which they remained roughly constant. For the 300 kDa membrane, permeate fluxes decreased when nonionic surfactant concentration increased, before a constant permeate flux was achieved at 2 $\times$ CMC. Surfactant adsorption on the membrane surface was not the main phenomenon of membrane fouling on UF of these emulsions, because the oil droplets and membrane surface are negatively charged. However, the zeta potential absolute value of oil droplets decreased when nonionic surfactant concentration increased (Fig. 1b). Hence, repulsion between charged oil droplets decreased and the cake resistance increased as a result of droplets approach.

As shown in Figs. 3c and 4c, for the UF of O/W emulsions stabilized with a cationic surfactant (CTAB) the permeate flux varied linearly with TMP, which means that concentration polarization is not significant. However, permeate fluxes were lower than those obtained with anionic and nonionic surfactants. As mentioned, the isoelectric point of membrane active layer is about 4, and membrane surface was negatively charged at the pH value of cationic surfactant-stabilized emulsions (pH ~ 7.5). Zeta potential measurements indicate that oil droplets are positively charged (Fig. 1b) and that electrostatic interactions

enhance surfactant adsorption on membrane surface. The hydrophilic head of cationic surfactant attaches to the negatively-charged membrane surface and the hydrophobic tails are oriented towards the bulk phase, increasing hydrophobicity on the surface, and reducing permeate flux through the membrane [37,40]. Even though permeate flux is quite low, it still depends on TMP. Zeta potential values are high and repulsive interaction between oil droplets hinders their deposition and therefore cake layer formation. Unlike anionic and nonionic surfactant-stabilized emulsions, permeate fluxes of cationic surfactant-stabilized emulsions are higher for the 300 kDa than for the 50 kDa membrane for all surfactant concentrations. These results confirm that electrostatic attraction between membrane surface and oil droplets plays an important role in flux reduction and it does not depend so much on the transport of solutes (oil and micelles) towards the membrane.

In addition, permeate flux reduction was higher at low CTAB concentration, reaching a minimum flux around 0.25–0.5 × CMC. Permeate fluxes were roughly constant at CTAB concentrations above CMC. Electrostatic attraction between the negatively charged membrane and the CTAB monomers at the lowest concentration (0.25 × CMC) led to a coverage of the membrane by a surfactant monolayer, which increased its hydrophobicity [37]. At higher CTAB concentrations, and once the monolayer was completed, surfactant aggregates started to form. These structures, known as “hemimicelles” [40], are formed beyond a critical concentration below the CMC, which is known as critical hemimicelle concentration (CHMC). CTAB monomers in hemimicelles are oriented with the charged head towards bulk phase increasing surface hydrophilicity. Another possible explanation is that cationic surfactants adsorbed onto the membrane surface modify membrane charge becoming less negative. Therefore, at high cationic surfactant concentrations the attraction of positively charged oil droplets for the membrane is lower, which leads to a reduced resistance due to droplet accumulation near the membrane surface.

3.2. Solute concentration in permeate

The average solute (oil and surfactant) concentration in permeate at different feed concentrations for the three surfactant-stabilized emulsions is shown in Fig. 5. Permeate concentration increased as surfactant concentration in feed emulsion increased for both membranes until a concentration close to CMC was reached. Above CMC, surfactant monomers concentration in the feed remained roughly constant (very close to CMC), even if additional surfactant was added. Whereas surfactant monomers can pass freely through membrane pores, micelles formed above CMC have a diameter in the same order of magnitude that membrane pore diameter and their permeation through the membrane is hindered.

Because of concentration polarization, which took place in UF of nonionic surfactant-stabilized emulsions, the solute content in permeate increased when surfactant concentration in feed was above CMC. This increase was specially marked for the 300 kDa membrane in which concentration polarization becomes more important.

Solute concentration in permeate for cationic surfactant-stabilized emulsion was higher because of its higher CMC, and also because electrostatic interactions with the membrane enhanced surfactant permeation [41].

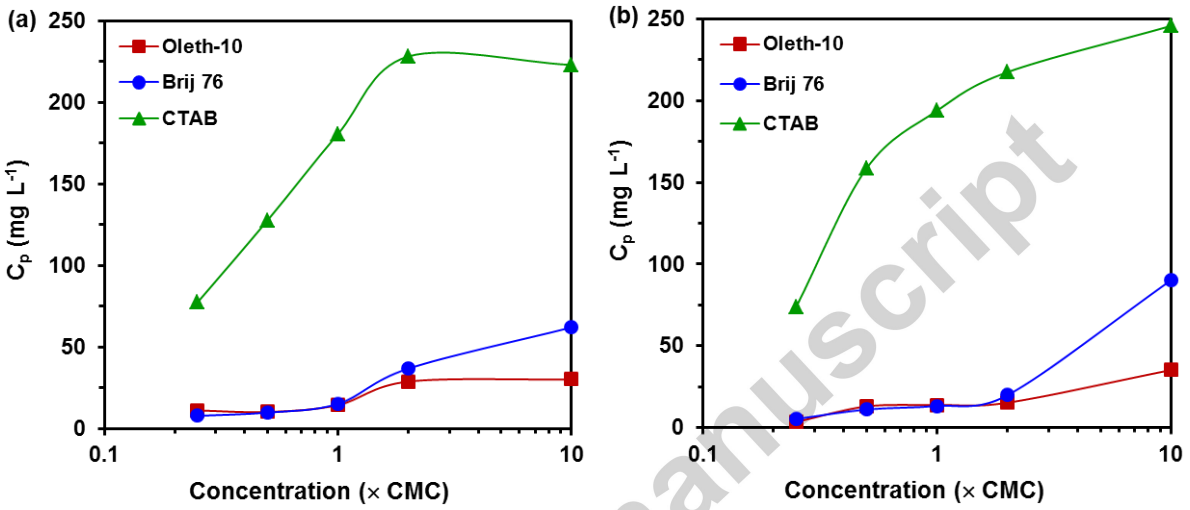

Figure 5. Solute concentration in permeate at varying surfactant concentration for UF of the three surfactant-stabilized O/W emulsions using: (a) 50 kDa, and (b) 300 kDa ceramic membranes.

Ceramic membranes have marked hydrophilic character and thus, electrostatic interaction may have a significant impact on surfactant adsorption on the surface. The active layer of ceramic membranes was negatively charged (ZrO^-/TiO^-) at pH values of O/W emulsions used in this work (6.5–7.5), and electrical repulsion prevented anionic and nonionic surfactant adsorption. Therefore, colloidal deposition of oil droplets or accumulation of micelles near the membrane surface might be the reason for flux decline due to membrane fouling in UF of anionic and nonionic surfactant-stabilized emulsions. However, for cationic surfactant-stabilized emulsion, surfactant adsorption on membrane surface and pore walls by electrostatic interactions are of major importance.

Experimental results shown in Fig. 5 indicated that oil permeation through the membrane was negligible and solute concentration in permeate was mainly due to surfactant monomers. Rejections based on COD of 97.7–99.4%, 98.6–99.7%, and 95.3–97.7% for anionic, nonionic, and cationic surfactant-stabilized emulsions, respectively, were achieved.

3.3. UF modeling of O/W emulsions stabilized with a nonionic surfactant (Brij 76)

A program written in Fortran has been used to perform model calculations. The program structure for the two models (A and B) developed to study UF of O/W emulsions stabilized with Brij 76 nonionic surfactant is shown in Fig. 6.

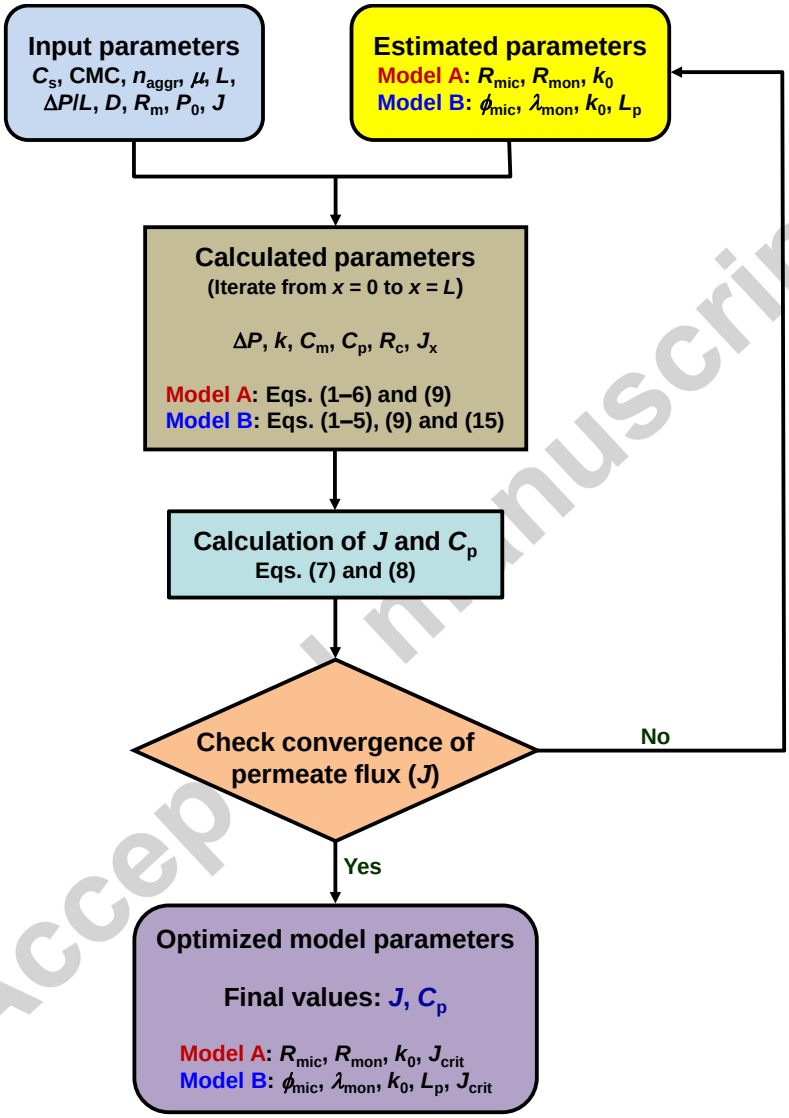

Figure 6. Logic diagram for UF models.

3.3.1. Model A

In a previous work [31] a model was reported to study the UF of a nonionic surfactant (Triton X-100) in order to avoid the influence of electrostatic interactions. This model (model A) has been extended in this research to O/W emulsions, using a nonionic surfactant (Brij 76) as emulsion stabilizer.

Table 1 shows the parameters obtained using the model described in Section 2.6, Eqs. (1–9), for the 300 kDa ceramic membrane. Model A predicted data and experimental data are shown in Fig. 7, showing a high correlation. However, at 0.25 × CMC the predicted solute concentration in permeate is significantly higher than the experimental value. This can be explained because the surfactant concentration used in this model is the initial concentration on emulsion. However, surfactant is partially adsorbed at the surface of emulsion droplets forming micelles, and therefore the surfactant concentration available as monomers in solution is lower. This fact is not significant at high initial surfactant concentrations, since the adsorbed amount by oil droplets is rather low compared to the initial concentration. This might also explain the higher rejections obtained at lower surfactant concentrations.

Table 1. Parameters obtained with model A for UF of O/W emulsions stabilized with a nonionic surfactant (Brij 76) using the 300 kDa ceramic membrane.

Feed surfactant concentration	R_{mic}	R_{mon}	k_0 (L m^{-2} h^{-1})	J_{crit} (L m^{-2} h^{-1})	R^2
0.25 × CMC	0.99990	0.91	19.5	233	0.9936
0.5 × CMC	0.99990	0.95	19.5	184	0.9901
1 × CMC	0.99985	0.95	19.5	181	0.9857
2 × CMC	0.99995	0.90	19.5	125	0.9479
10 × CMC	0.99960	0.70	19.5	106	0.9578

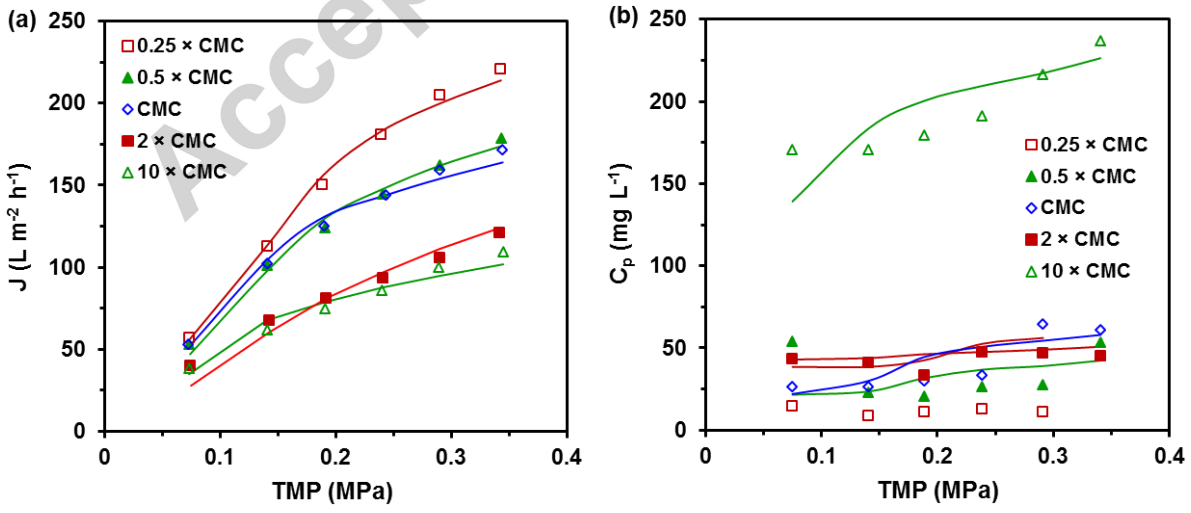

Figure 7. Permeate flux (a) and solute concentration in permeate (b) at different TMP and Brij 76 concentrations for UF of a model O/W emulsion using a 300 kDa ceramic membrane. Experimental data (symbols) and model A predictions (lines) using parameters from Table 1.

The mass transfer coefficient is constant for the tested surfactant concentration range and for both membranes (Tables 1 and 2), as expected since it depends on hydrodynamic conditions as well as on rheological properties of the solution.

The critical flux, J_{crit}, shown in Tables 1 and 2 predicted by the model decreases as feed surfactant concentration increases. The mean droplet size of emulsions formulated with a nonionic surfactant decreases when feed surfactant concentration increases (Fig. 1a). This leads to oil deposition on the membrane surface, since forces that tend to move the oil droplets away from the surface are weaker [42]. Moreover, zeta potential absolute value decreases at higher feed surfactant concentrations (Fig. 1b), resulting in lower repulsion among droplets. As J_{crit} depends on feed properties and hydrodynamic conditions, their values should be similar for the different feed surfactant concentrations because the hydrodynamic conditions used in this study are very similar for both types of membranes. J_{crit} was very low at 0.5 × CMC feed surfactant concentration using the 300 kDa membrane, while for the 50 kDa membrane this critical flux was not reached at 0.25 × CMC and 0.5 × CMC (Table 2).

Table 2. Parameters obtained with model A for UF of O/W emulsions stabilized with a nonionic surfactant (Brij 76) using the 50 kDa ceramic membrane.

Feed surfactant concentration	R_{mic}	R_{mon}	k_0 (L m^{-2} h^{-1})	J_{crit} (L m^{-2} h^{-1})	R^2
0.25 × CMC	0.99995	0.98	19.5	>220	0.9974
0.5 × CMC	0.99995	0.96	19.5	>220	0.9912
1 × CMC	0.99995	0.93	19.5	195	0.9947
2 × CMC	0.99995	0.80	19.5	139	0.9880
10 × CMC	0.99995	0.70	19.5	110	0.9932

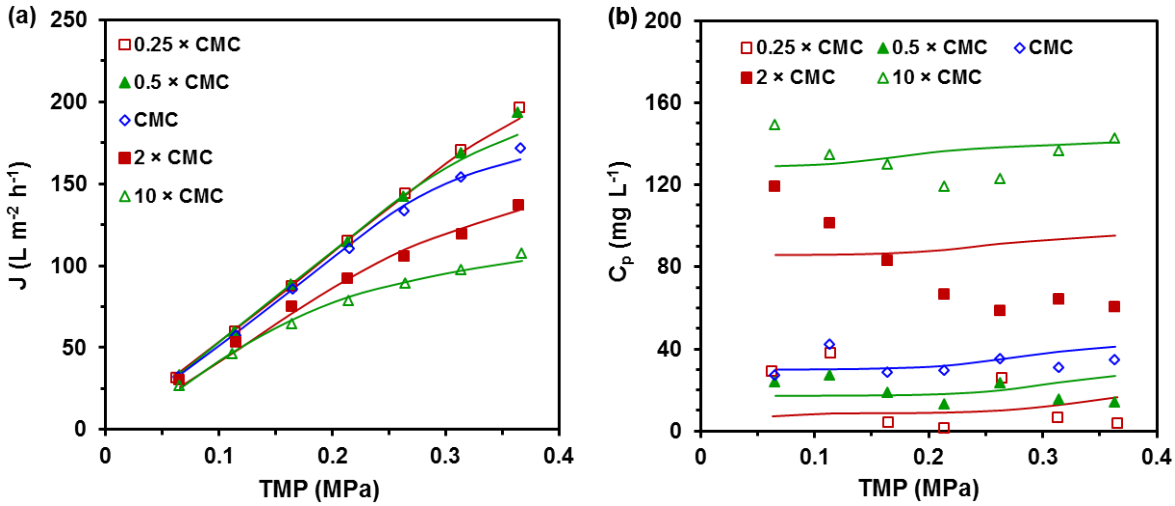

Figure 8. Permeate flux (a) and solute concentration in permeate (b) at different TMP and Brij 76 concentrations for UF of a model O/W emulsion using a 50 kDa ceramic membrane. Experimental data (symbols) and model A predictions (lines) using parameters from Table 2.

Model A predicted data using parameters from Table 2 and experimental data for the 50 kDa ceramic membrane are given in Fig. 8a, showing a good correlation. However, it can be observed in Fig. 8b that the experimental solute concentration in permeate decreases initially with TMP (and therefore with permeate flux), remaining constant or even increasing at higher feed surfactant concentrations due to concentration polarization. This decrease in permeate concentration is mainly caused by diffusion and convection phenomena that take place inside the membrane pores [43–45].

3.3.2. Model B

A new equation, based on hydrodynamic models, should be used to take into account the aforementioned phenomena [43]:

$$J_s = K_c J C_s - K_d D \frac{dC_s}{dz} \qquad (10)$$

where J_s is the solute flux (JC_p), K_c and K_d are the hindrance factors for convective and diffusive fluxes, respectively, D is the solute diffusion coefficient, and C_s is the solute concentration. Eq. (10) can be integrated through the membrane pore taking into account the equilibrium partition coefficient defined by [43]:

$$\phi = \frac{C_{s(z=0)}}{C_m} = \frac{C_{s(z=L_p)}}{C_p} \qquad (11)$$

where L_p is the pore length. Integration leads to Eq. (12) in terms of the actual sieving coefficient (S_a), that correlates the solute concentration in permeate (C_p) and on membrane surface (C_m) [43]:

$$S_a = \frac{C_p}{C_m} = \frac{S_\infty \exp(Pe_m)}{S_\infty + \exp(Pe_m) - 1} \quad (12)$$

$$Pe_m = \frac{K_c J L_p}{K_d D} \quad (13)$$

$$S_\infty = K_c \phi \quad (14)$$

These equations were developed for diffusion and convection of rigid solutes in cylindrical pores [44]. As experimental permeate concentrations are lower than CMC in this study, Eqs. (12–14) may be used assuming that there is no transport of micelles through the membrane pores. Micelles concentration on membrane surface, $C_{mic,m}$, will affect surfactant concentration inside the membrane pores, i.e., will affect the partition coefficient relative to membrane side. Therefore, Eq. (12) becomes:

$$C_p = \frac{(n_{aggr}\phi_{mic}C_{mic,m} + CMC\,\phi)\exp(Pe_m)}{S_\infty + \exp(Pe_m) - 1} \quad (15)$$

K_c, K_d and ϕ values for surfactant monomers can be obtained with the following equations, valid for spheres without interaction:

$$\phi = (1-\lambda)^2 \quad (16)$$

$$K_c = (2-\phi)(1 - 0.255\lambda - 1.279\lambda^2 + 1.035\lambda^3) \quad (17)$$

$$K_d = 1 - 2.30\lambda + 1.154\lambda^2 + 0.224\lambda^3 \quad (18)$$

where λ is the ratio between solute radius and membrane pore radius.

Taking into account these previous considerations, a new model (model B) was developed to better fit solute concentration in permeate. In model B three new fit parameters were considered instead of R_{mic} and R_{mon}: (a) the equilibrium partition coefficient for the micelles (ϕ_{mic}), (b) the ratio between surfactant monomer radius and membrane pore radius (λ_{mon}), and (c) the membrane pore length (L_p). In this new model Eq. (15) was used instead

of Eq. (6) in the program to estimate C_p. Results obtained for the 300 kDa ceramic membrane are shown in Table 3 and Fig. 9.

Table 3. Parameters obtained with model B for the UF of O/W emulsions stabilized with a nonionic surfactant (Brij 76) using the 300 kDa ceramic membrane.

Feed surfactant concentration	ϕ_{mic}	λ_{mon}	k_0 (L m^{-2} h^{-1})	L_p (m)	J_{crit} (L m^{-2} h^{-1})	R^2
0.25 × CMC	0.00001	0.85	19.5	3×10^{-6}	238	0.9613
0.5 × CMC	0.00003	0.80	19.5	0.5×10^{-6}	182	0.9893
1 × CMC	0.00012	0.80	19.5	0.7×10^{-6}	180	0.9833
2 × CMC	0.00015	0.75	19.5	1×10^{-6}	125	0.9503
10 × CMC	0.00030	0.55	19.5	7×10^{-6}	106	0.9568

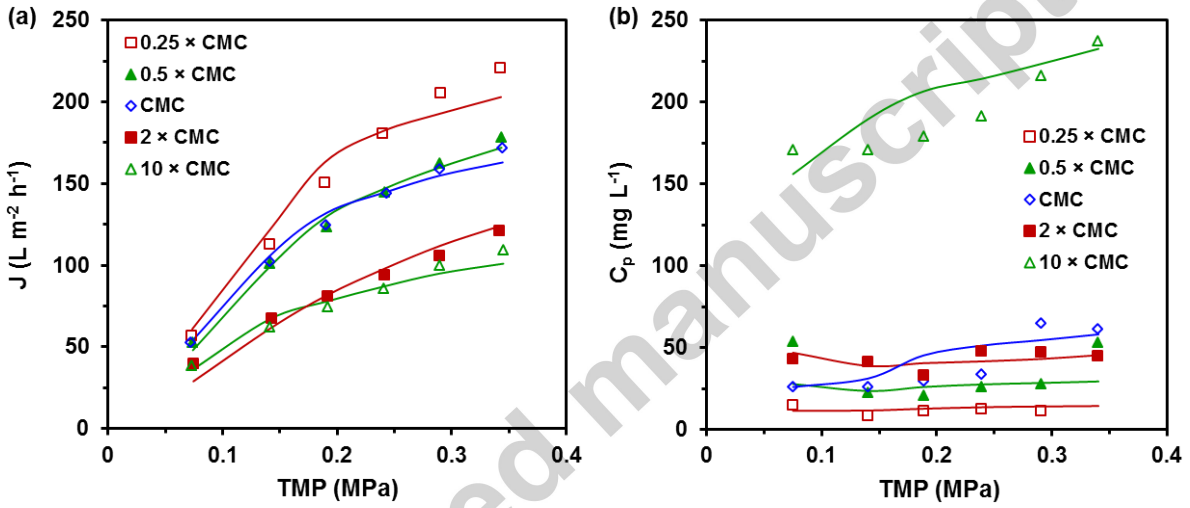

Figure 9. Permeate flux (a) and solute concentration in permeate (b) at different TMP and Brij 76 concentrations for UF of a model O/W emulsion using a 300 kDa ceramic membrane. Experimental data (symbols) and model B predictions (lines) using parameters from Table 3.

Fig. 9 shows an improved fit of experimental data for C_p, but a poorer fit of permeate fluxes at 0.25 × CMC feed surfactant concentration (R^2 changed from 0.9936 to 0.9613).

Results obtained for the 50 kDa membrane are shown in Table 4 and Fig. 10. In this case, a better fit is achieved for both C_p and permeate flux.

Table 4. Parameters obtained with model B for the UF of O/W emulsions stabilized with a nonionic surfactant (Brij 76) using the 50 kDa ceramic membrane.

Feed surfactant concentration	ϕ_{mic}	λ_{mon}	k_0 (L m^{-2} h^{-1})	L_p (m)	J_{crit} (L m^{-2} h^{-1})	R^2
0.25 × CMC	0.00001	0.85	19.5	1×10^{-6}	>220	0.9970

0.5 × CMC	0.00001	0.80	19.5	1×10^{-6}	>220	0.9906
1 × CMC	0.00005	0.78	19.5	0.7×10^{-6}	195	0.9946
2 × CMC	0.00005	0.70	19.5	0.6×10^{-6}	139	0.9882
10 × CMC	0.00010	0.60	19.5	3×10^{-6}	110	0.9928

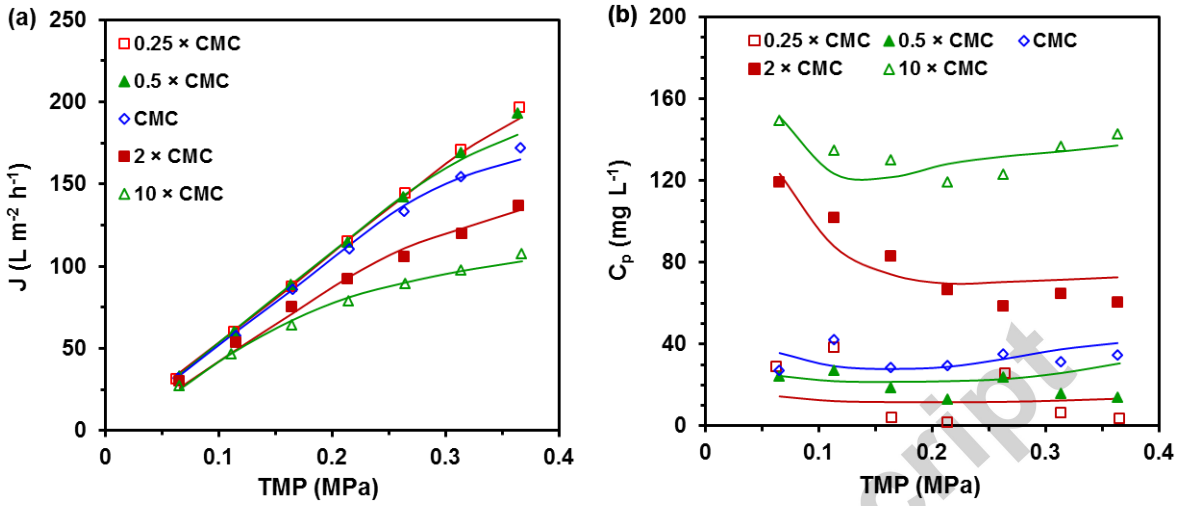

Figure 10. Permeate flux (a) and solute concentration in permeate (b) at different TMP and Brij 76 concentrations for UF of a model O/W emulsion using 50 kDa ceramic membrane. Experimental data (symbols) and model B predictions (lines) using parameters from Table 4.

4. Conclusions

Experimental results for the UF of surfactant-stabilized O/W emulsions formulated in this work indicate that oil permeation through the membrane was negligible. Solute concentration in permeate was mainly due to surfactant monomers: COD rejections higher than 95% were achieved for both tubular ceramic membranes tested.

Electrostatic interaction plays an important role on permeate flux and solute rejection. When membrane surface and emulsion droplets have the same charge sign, electrostatic repulsion hinders surfactant (and charged oil droplets) adsorption on the membrane and its leakage across it, decreasing concentration polarization and cake layer formation, and thus increasing permeate flux. However, if membrane surface and emulsion droplets have an opposite sign, electrostatic attraction helps adsorption and transport of surfactant. It causes pore blocking and hydrophobicity increase on membrane surface. Permeate flux diminishes.

Emulsion physicochemical properties have influence on fouling characteristics: high zeta potential values enhance repulsion between oil droplets and permeate flux increases as a result of cake porosity increase; likewise, emulsion ionic strength increases with surfactant

concentration, which favors coagulation and compaction of cake layer, decreasing permeate flux.

UF modeling of nonionic surfactant-stabilized O/W emulsions was first performed (Model A) using osmotic pressure model and film theory by defining two different types of rejection, taking into account that surfactants are present both as free monomers and micelles. Experimental permeate fluxes were similar to those predicted by Model A, with a high correlation for both membranes. However, high deviations were observed concerning solute concentrations in permeate, especially for the 50 kDa membrane.

Therefore, three new adjustment parameters were used in a second model (Model B) to account for diffusion and convection phenomena inside membrane pores, achieving a better prediction of solute concentration in permeates of both membranes.

Acknowledgments

The zeta potential equipment used in this work was co-financed by the Consejería de Educación y Ciencia del Principado de Asturias (Plan I+D+i 2001–2004, Ref.: COF04-50).

References

[1] M. Greeley, N. Rajagopalan, Impact of environmental contaminants on machining properties of metalworking fluids, Tribol. Int. 37 (2004) 327–332.

[2] J.M. Benito, A. Cambiella, A. Lobo, G. Gutiérrez, J. Coca, C. Pazos, Formulation, characterization and treatment of metalworking oil-in-water emulsions, Clean Technol. Environ. Policy 12 (2010) 31–41.

[3] A. Cambiella, J.M. Benito, C. Pazos, J. Coca, A. Hernández, J.E. Fernández, Formulation of emulsifiable cutting fluids and extreme pressure behavior, J. Mater. Process. Technol. 184 (2007) 139–145.

[4] P. Cañizares, F. Martínez, E. Jiménez, C. Sáez, M.A. Rodrigo, Coagulation and electrocoagulation of oil-in-water emulsions, J. Hazard. Mater. 151 (2008) 44–51.

[5] D. Allende, A. Cambiella, J.M. Benito, C. Pazos, J. Coca, Destabilization-enhanced centrifugation of metalworking oil-in-water emulsions: effect of demulsifying agents, Chem. Eng. Technol. 31 (2008) 1007–1014.

[6] J.L. Kenneth, Demulsification: Industrial Applications, Marcel Dekker, New York, 1983.

[7] B. Chakrabarty, A.K. Ghoshal, M.K. Purkait, Ultrafiltration of stable oil-in-water emulsion by polysulfone membrane, J. Membr. Sci. 325 (2008) 427–437.

[8] A. Lobo, A. Cambiella, J.M. Benito, C. Pazos, J. Coca, Ultrafiltration of oil-in-water emulsions with ceramic membranes: influence of pH and crossflow velocity, J. Membr. Sci. 278 (2006) 328–334.

[9] D. Vasanth, G. Pugazhenthi, R. Uppaluri, Cross-flow microfiltration of oil-in-water emulsions using low cost ceramic membranes, Desalination 320 (2013) 86–95.

[10] N. Ghaffour, M.W. Naceur, N. Drouiche, H. Mahmoudi, Use of ultrafiltration membranes in the treatment of refinery wastewaters, Desalin. Water Treat. 5 (2009) 159–166.

[11] V. Singh, M.K. Purkait, C. Das, Cross-flow microfiltration of industrial oily wastewater: Experimental and theoretical consideration, Sep. Sci. Technol. 46 (2011) 1213–1223.

[12] D. Lu, T. Zhang, J. Ma, Ceramic membrane fouling during ultrafiltration of oil/water emulsions: roles played by stabilization surfactant of oil droplets, Environ. Sci. Technol. 49 (2015) 4235–4244.

[13] G. Gutiérrez, J.M. Benito, J. Coca, C. Pazos, Vacuum evaporation of waste oil-in-water emulsions from a copper metalworking industry, Ind. Eng. Chem. Res. 48 (2009) 2100–2106.

[14] G. Gutiérrez, J.M. Benito, J. Coca, C. Pazos, Vacuum evaporation of surfactant solutions and oil-in-water emulsions, Chem. Eng. J. 162 (2010) 201–207.

[15] G. Gutiérrez, J.M. Benito, J. Coca, C. Pazos, Evaporation of aqueous dispersed systems and concentrated emulsions formulated with non-ionic surfactants, Int. J. Heat Mass Transf. 69 (2014) 117–128.

[16] H. Bataller, S. Lamaallam, J. Lachaise, A. Gracia, C. Dicharry, Cutting fluid emulsions produced by dilution of a cutting fluid concentrate containing a cationic/nonionic surfactant mixture, J. Mater. Process. Technol. 152 (2004) 215–220.

[17] J.M. Benito, G. Ríos, B. Gutiérrez, C. Pazos, J. Coca, Integrated process for the removal of emulsified oils from effluents in the steel industry, Sep. Sci. Technol. 34 (1999) 3031–3043.

[18] M. Matos, C.F. García, M.A. Suárez, C. Pazos, J.M. Benito, Treatment of oil-in-water emulsions by a destabilization/ultrafiltration hybrid process: statistical analysis of operating parameters, J. Taiwan Inst. Chem. Eng. 59 (2016) 295–302.

[19] D. Abdessemed, G. Nezzal, R. Ben Aim, Coagulation-adsorption-ultrafiltration for wastewater treatment and reuse, Desalination 131 (2000) 307–314.

[20] D. Allende, D. Pando, M. Matos, C.E. Carleos, C. Pazos, J.M. Benito, Optimization of a membrane hybrid process for oil-in-water emulsions treatment using Taguchi experimental design, Desalin. Water Treat. 57 (2016) 4832–4841.

[21] G. Gutiérrez, A. Lobo, D. Allende, A. Cambiella, C. Pazos, J. Coca, J.M. Benito, Influence of coagulant salt addition on the treatment of oil-in-water emulsions by centrifugation, ultrafiltration, and vacuum evaporation, Sep. Sci. Technol. 43 (2008) 1884–1895.

[22] G. Gutiérrez, A. Lobo, J.M. Benito, J. Coca, C. Pazos, Treatment of a waste oil-in-water emulsion from a copper-rolling process by ultrafiltration and vacuum evaporation, J. Hazard. Mater. 185 (2011) 1569–1574.

[23] T. Mohammadi, A. Esmaeelifar, Wastewater treatment of a vegetable oil factory by a hybrid ultrafiltration-activated carbon process, J. Membr. Sci. 254 (2005) 129–137.

[24] A. Lobo, A. Cambiella, J.M. Benito, C. Pazos, J. Coca, Effect of a previous coagulation stage on the ultrafiltration of a metalworking emulsion using ceramic membranes, Desalination 200 (2006) 330–332.

[25] Y. Yang, R. Chen, W. Xing, Integration of ceramic membrane microfiltration with powdered activated carbon for advanced treatment of oil-in-water emulsion, Sep. Purif. Technol. 76 (2011) 373–377.

[26] E. Fernández, J.M. Benito, C. Pazos, J. Coca, I. Ruiz, G. Ríos, Regeneration of an oil-in-water emulsion after use in an industrial copper rolling process, Colloid Surf. A-Physicochem. Eng. Asp. 263 (2005) 363–369.

[27] M. Matos, A. Lobo, E. Fernández, J.M. Benito, C. Pazos, J. Coca, Recycling of oily ultrafiltration permeates to reformulate O/W emulsions, Colloid Surf. A-Physicochem. Eng. Asp. 331 (2008) 8–15.

[28] J. Altmann, S. Ripperger, Particle deposition and layer formation at the crossflow microfiltration, J. Membr. Sci. 124 (1997) 119–128

[29] P. Harmant, P. Aimar, Coagulation of colloids in a boundary layer during cross-flow filtration, Colloid Surf. A-Physicochem. Eng. Asp. 138 (1998) 217–230.

[30] A.-S. Jönsson, B. Jönsson, Ultrafiltration of colloidal dispersions–A theoretical model of the concentration polarization phenomena, J. Colloid Interface Sci. 180 (1996) 504–518.

[31] A.-S. Jönsson, B. Jönsson, H. Byhlin, A concentration polarization model for the ultrafiltration of nonionic surfactants, J. Colloid Interface Sci. 304 (2006) 191–199.

[32] T.F. Tadros, B. Vincent, Liquid/liquid interfaces, in: P. Becher (Ed.), Encyclopedia of Emulsion Technology, Vol. 1, Marcel Dekker Inc., New York, 1983, pp. 1–56.

[33] L.H. Keith, Compilation of EPA's Sampling and Analysis Methods, CRC Press, London, 1996.

[34] J.H. Markels, S. Lynn, C.J. Radke, Cross-flow ultrafiltration of micellar surfactant solutions, AIChE J. 41 (1995) 2058–2066.

[35] V.S. Minnikanti, S. DasGupta, S. De, Prediction of mass transfer coefficient with suction for turbulent flow in cross flow ultrafiltration, J. Membr. Sci. 157 (1999) 227–239.

[36] N. Nabi, P. Aimar, M. Meireles, Ultrafiltration of an olive oil emulsion stabilized by an anionic surfactant, J. Membr. Sci. 166 (2000) 177–188.

[37] E. Fernández, J.M. Benito, C. Pazos, J. Coca, Ceramic membrane ultrafiltration of anionic and nonionic surfactant solutions, J. Membr. Sci. 246 (2005) 1–6.

[38] Y. Zhao, W. Xing, N. Xu, F.-S. Wong, Effects of inorganic electrolytes on zeta potentials of ceramic microfiltration membranes, Sep. Purif. Technol. 42 (2005) 117–121.

[39] J. Mueller, Y. Cen, R.H. Davis, Crossflow microfiltration of oily water, J. Membr. Sci. 129 (1997) 221–235.

[40] S. Paria, K.C. Khilar, A review on experimental studies of surfactant adsorption at the hydrophilic solid-water interface, Adv. Colloid Interface Sci. 110 (2004) 75–95.

[41] P. Tounissou, M. Hebrant, C. Tondre, On the behavior of micellar solutions in tangential ultrafiltration using mineral membranes, J. Colloid Interface Sci. 183 (1996) 491–497.

[42] S.-H. Yoon, C.-H. Lee, K.-J. Kim, A.G. Fane, Three-dimensional simulation of the deposition of multi-dispersed charged particles and prediction of resulting flux during cross-flow microfiltration, J. Membr. Sci. 161 (1999) 7–20.

[43] W.S. Opong, A.L. Zydney, Diffusive and convective protein through asymmetric membranes, AIChE J. 37 (1991) 1497–1510.

[44] W.M. Deen, Hindered transport of large molecules in liquid-filled pores, AIChE J. 33 (1987) 1409–1423.

[45] S. Bhattacharjee, A. Sharma, P.K. Bhattacharya, Estimation and influence of long range solute. Membrane interactions in ultrafiltration, Ind. Eng. Chem. Res. 35 (1996) 3108–3121.

Highlights

- Surfactant effect on ultrafiltration (UF) of O/W emulsions investigated
- Three types of surfactant (anionic, nonionic and cationic) studied
- UF modeling of nonionic surfactant-stabilized O/W emulsion performed
- Two types of rejection defined regarding surfactant free monomers and micelles
- Improved fit considering diffusion/convection effects inside membrane pores

Graphical abstract